

# Functional mapping of regional airway obstruction and gas trapping in 3D using dynamic HP He-3 MRI

J. Dai<sup>1</sup>, E. T. Peterson<sup>2</sup>, J. H. Holmes<sup>3</sup>, R. V. Cadman<sup>1</sup>, R. L. Sorkness<sup>4</sup>, and S. B. Fain<sup>1,5</sup>

<sup>1</sup>Medical Physics, University of Wisconsin - Madison, Madison, Wisconsin, United States, <sup>2</sup>Biomedical Engineering, University of Wisconsin - Madison, Madison, Wisconsin, United States, <sup>3</sup>Global Applied Science Laboratory, GE Healthcare, Madison, Wisconsin, United States, <sup>4</sup>pharmacy, University of Wisconsin - Madison, Madison, Wisconsin, United States, <sup>5</sup>Radiology, University of Wisconsin - Madison, Madison, Wisconsin, United States

**Introduction:** Hyperpolarized noble gas MRI enables high contrast to noise dynamic imaging during respiratory maneuvers. Gas in-flow during inhalation and out-flow during exhalation within a localized lung area are important parameters that reflect regional ventilation and severity of airway obstruction. This work presents two modeling approaches to quantify regional airway obstruction during inhalation and during forced exhalation using dynamic hyperpolarized helium-3 (HP <sup>3</sup>He) MR images acquired by a 3D Multi-Echo-PR (ME-VIPR) acquisition [1].

**Methods:** MRI and modeling were performed in 6 subjects: two healthy normal adults, two adults with known ventilation defects, a healthy normal child, and a child with known ventilation defects and asthma using a 1.5 T clinical scanner equipped with broadband capability (GE HealthCare, Milwaukee, WI, USA). Images were acquired using a rigid birdcage coil (Rapid Biomedical, Würzburg-Rimpar, Germany) tuned to ~48 MHz. A ME-VIPR acquisition was performed using a cubic 42 cm FOV, with 3 full echoes and 2 half echoes acquired per TR, and ramp sampling with maximum radial distance from the center in k-space corresponding to 64 evenly spaced points on a Cartesian grid. During imaging, subjects performed a 4 s inspiration maneuver followed by a breath-hold of 14% of total lung capacity of HP <sup>3</sup>He for approximately 10 s concluding with a forced exhalation followed by normal breathing of room air for the remaining scan duration.

**Reconstruction:** Data from the 3D dynamic scan were reconstructed in 1-second time frames throughout the ~60 s long acquisition using six iterations of the Iterative HYPR (I-HYPR) [2] algorithm using an 8-second sliding window composite.

**Relative inspiratory gas flow:** The signal in a region of interest was measured in the trachea through the time course of inhalation to estimate the tracheal input function (TIF). The signal decay was corrected for both  $T_1$  and RF effects using an exponential curve fit to the signal decay during the breath-hold period. A singular value decomposition (SVD) algorithm [3] was applied to deconvolve the TIF from signals in the parenchyma on a voxel by voxel basis to provide a residence time curve,  $R(t)$ . This results in a regional uptake image without the effects of the inhalation. The relative inspiratory flow measure for each voxel was then calculated by recording the maximum value of the  $R(t)$ ,  $R_{\max}$ .  $R_{\max}$  measures the gas flow within one specific voxel after a unit gas flow is delivered at the trachea.

**Washout and gas trapping quantification:** The washout delay time was calculated semi-quantitatively as the time interval between the maximum signal at end of breath-hold and 50% of the maximum signal during the forced exhalation on a voxel by voxel basis to depict regional gas-trapping as a parametric map.

**Results and Discussion:** Figure 1 (a - f) shows a typical example of the relative flow maps for the six subjects analyzed. Normal subjects I, II & V demonstrate higher relative gas flow in the large airways, and reduced but comparatively homogeneous flow in the lung parenchyma. However, the healthy normal subject I with fast inhalation (Fig. 1a) demonstrates higher values of relative flow and regional heterogeneity compared to subject II with slow inhalation (Fig. 1b). This is unexpected because the deconvolution should account for the differences in the input function which leads us to believe that this is possibly due to dynamic equilibrium effects and underestimation of the TIF of subject I as a result of intravoxel dephasing. For subjects III, IV & VI with known ventilation defects, heterogeneity is also observed in the relative flow map (Arrows in Fig. 1), especially in areas of greater flow as gas is redirected away from obstructed regions. Subjects IV & VI are asthmatics showing patchy distribution of low and high flow as a result of local redirection of flow due to multiple areas of obstruction. In subject III increased flow is more specific to a focal region in the right upper lobe due to obstruction of the neighboring parenchyma caused by a pulmonary vascular aneurysm seen as an area of gas trapping in Fig. 1i. Forced expiratory volume in 1 s percent predicted (FEV1%pred) reasonably correlated with our results except that FEV1%pred for subject IV (111%) suggested no obvious obstruction when imaging abnormalities are apparent. Figure 1 (g - l) shows the corresponding washout delay maps for the identical coronal slices intended as a semi-quantitative regional map of gas trapping during forced exhalation. Abnormally long washout delays during forced exhalation are especially prominent for the subject with severe asthma (IV) with a regionally heterogeneous pattern similar to, but distinct from, the pattern of relative flow (Fig. 1j). More mild gas trapping is observed in the right middle and lower lobes of subject VI with childhood asthma. However, regions of delayed washout are also noted for the healthy normal subjects, especially subject II with a prolonged TIF, which suggests that further standardization, perhaps in conjunction with spirometry, is needed to compensate for variations in ability to perform the forced exhalation maneuver. RV/TLC data for subject IV & VI (0.45 & 0.35 respectively) measured by plethysmography were higher than for the other subjects (0.26-0.28), consistent with the washout delay results with the exception of subject II as previously mentioned.

**Conclusion:** We have demonstrated two methods to provide quantitative 3D parametric maps of airway obstruction and trapping using dynamic HP <sup>3</sup>He MRI. These methods allow measurement of relative degree of airway obstruction and the regional associations between effected lung regions. Future work will extend the use of quantitative modeling in these data to improve regional normalization and to explore changes in lung compliance.

**References:** [1] Holmes, et al. Magn Reson Med 2008 [2] O'Halloran, et al. Magn Reson Med 2008 [3] Salluzzi, et al. Magn Reson Imag 2005

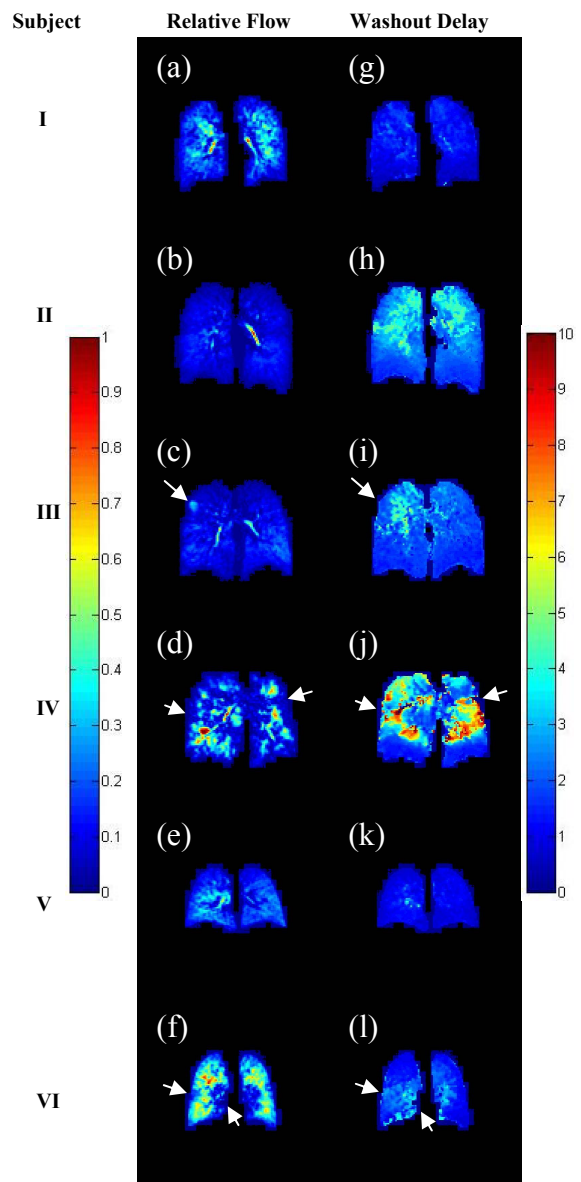


**Figure 1: Comparison of relative flow map (left column) and washout delay map (right column) between different subjects.** (I) Healthy adult with fast inhalation. (II) Healthy adult with slow inhalation. (III) Adult with right upper lobe obstruction due to pulmonary aneurysm. (IV) Adult with severe asthma. (V) Healthy child. (VI) Child with asthma. Left colorbar indicates  $R_{\max}$  and right colorbar indicates delay in seconds. Arrows in figure point out abnormalities demonstrated in the parametric maps.